UNIVERSIDAD DE CONCEPCIÓN
FACULTAD DE CIENCIAS FÍSICAS Y MATEMÁTICAS

THE ORIGINS OF ULTRA DIFFUSE GALAXIES: CHARACTERIZATION OF THEIR GLOBULAR CLUSTER POPULATION

Por: Pablo Astudillo Sotomayor

Tesis presentada a la Facultad de Ciencias Fisicas y Matematicas de la Universidad de Concepción para optar al grado académico de Magíster en Ciencias con Mención en Astronomía

Enero 2025
Concepción, Chile

Profesores Guía: Nathan W. C. Leigh & Ricardo Demarco

AGRADECIMIENTOS

Quisiera comenzar agradeciendo profundamente a mi tutor, Dr. Nathan Leigh por su enseñanza, experiencia y apoyo durante la tesis. Trabajar con él en este proyecto ha sido de mucho aprendizaje a nivel profesional y humano. Le estaré eternamente agradecido por lo que me enseño en mi primer acercamiento a la investigación y su apoyo a continuar en ella. A mi co-tutor Dr. Ricardo Demarco, por el apoyo, el conocimiento y las discusiones, su compañía en mi primer congreso internacional la atesorare el resto de mi vida.

A mi familia, especialmente a mi madre María Elena Sotomayor González, quien desde temprana edad me incito siempre a cuestionar y analizar todo, hacer preguntas y buscar nuevos conocimientos cuando no tenia una respuesta. Por su constante apoyo y amor durante mi vida, que durante este periodo ha sido un pilar fundamental de fuerza para continuar adelante.

A mis amistades, por los buenos momentos día a día, las risas y la compañía durante estos años.

Resumen

Presentamos nuestro análisis de los sistemas de cúmulos globulares (GC) de seis galaxias ultra difusas (UDG) en diferentes entornos. Estudiamos cómo los procesos dinámicos podrían haber modelado la función de luminosidad de cúmulos globulares (GCLF). Comenzamos ajustando GCLF gaussianas y gaussianas sesgadas. Obtenemos la distribución espacial de los GCs y usamos observables fotométricos para modelar los perfiles de densidad, masa y dispersión de velocidad de las UDGs. Luego calculamos las escalas temporales de fricción dinámica y de disrupción para los GCs en cada UDG. Analizamos cómo la fricción dinámica (DF) y la disrupción podrían modelar la GCLF y la distribución espacial si las escalas temporales son menores a un tiempo de Hubble. La fricción dinámica actuaria principalmente sobre los GCs masivos de la GCLF haciéndolos hundirse, potencialmente creando un cúmulo estelar nuclear. Por otro lado, la disrupción afectaría principalmente a los GCs en el extremo de baja masa, estableciendo un limite inferior para la GCLF. Nuestros resultados son consistentes con las tendencias observables de los sistemas de GCs en las UDGs, como $R_{gc}/R_e < 1$ y una GCLF más estrecha. Finalmente, somos capaces de restringir los escenarios de formación consistentes con nuestras escalas temporales estimadas y la inexistencia de cúmulos estelares nucleares observada, incluso cuando los GCs tienen tiempos de fricción dinámica bajos.

Keywords – Cúmulos Globulares, Galaxias Ultra Difusas, Fricción Dinámica, Formación de Galaxias.

Abstract

We present our analysis of the globular cluster (GC) systems in six ultra diffuse galaxies (UDG) living in different environments, with the over-arching goal to understand the origins of UDGs. We study how dynamical processes may have shaped the GC luminosity functions (GCLFs) and their spatial distributions. We begin by fitting gaussian and skew-gaussian profiles to the GCLFs in order to evaluate if they are different from normal dwarf galaxies, for which a Gaussian profile typically matches the data. We retrieve the spatial distribution of GCs and use photometric observables to model the density, enclosed mass and velocity dispersion profiles. We then compute dynamical friction and disruption timescales for GCs in each UDG. We analyze how dynamical friction (DF) and disruption may have shaped the GCLFs and spatial distributions. DF would preferentially make the high-mass end of the GCLF sink into the center, potentially forming a nuclear star cluster and a skew Gaussian GCLF (positively skewed) profile that is depleted at the high-mass end. Disruption, on the other hand, would likely affect those GCs at the low-mass end of the GCLF, establishing a lower limit for GC mass and a negatively skew gaussian. Our results are consistent with observable trends of GC systems in UDGs, such as the distribution of Galactocentric radii, where $R_{gc}/R_e < 1$, and a narrower GCLF. Finally we are able to constrain formation scenarios consistent with our estimated timescales and the lack of nuclear star clusters, even in those galaxies with DF timescales shorter than a Hubble time.

Keywords – Globular Clusters, Ultra-Diffuse Galaxies, Dynamical Friction, Galaxy Formation.

Contents

List of Tables

List of Figures

Chapter 1

Introduction

1.1 Introduction

Ultra diffuse galaxies were recently discovered by van Dokkum et al. (2015a). These galaxies are defined as having a low surface brightness $\mu_e = 24 - 28\text{mag/arcsec}^2$ comparable to dwarf galaxies but effective radii much larger 0.8 kpc $< r_e <$ 5 kpc than those of dwarf galaxies. Thousands of UDGs have been identified in the Coma cluster (van Dokkum et al., 2015a,b; Yagi et al., 2016; Koda et al., 2015), the Virgo cluster (Mihos et al., 2015). Their dark matter content is known to be in the form of a low-mass cored halo (van Dokkum et al., 2016; Trujillo et al., 2017; Amorisco and Loeb, 2016; Di Cintio et al., 2017), They have old stellar populations and no signs of actual star formation, as inferred from the absence of H_α emission. These galaxies are situated on the red sequence of the color-magnitude diagram and with stellar masses between $10^7 < M_* < 10^8$ (Koda et al., 2015). These galaxies represent a strange but abundant type of galaxy in our Universe.

Several authors have proposed different origins or formation mechanisms for UDGs. We distinguish between formation mechanisms by defining them according to an in-situ/ex-situ nomenclature; an in-situ origin implies that no external processes are needed for their formation whereas an ex-situ origin requires the opposite. In-situ formation mechanisms include strong stellar feedback due to burst in star formation, Supernova feedback and gas outflows that end wiping out the gas of the galaxy and giving the UDGs their characteristic low gas and high effective radii. Ex-situ formation mechanisms occur in galaxy clusters/groups, or environments

where the local galaxy density is much higher than the Universal mean. These include ram pressure stripping when galaxies fall into the intra-cluster medium and find a higher density that can overcome their gas gravitational bound, tidal stripping from the interaction with massive galaxies, collisions between dwarf galaxies.

Di Cintio et al. (2017) and Chan et al. (2018) considered an in situ origin for UDGs by performing cosmological simulations of isolated field dwarf galaxies including feedback from supernovae and massive stars. This feedback acts to drive away the gas in outflows, causing bursts of star formation and giving rise to spatially extended stellar components, as observed in UDGs. In galaxy clusters and group environments, the presence of hot gas can stop star formation via tidal and gas stripping processes when the UDG progenitors infall into the galaxy cluster. This scenario constitutes an ex-situ formation mechanism, since internal processes do not form the basis for their formation, and instead environmental processes are responsible. Carleton et al. (2019) advocate an ex-situ origin, arguing that the stellar feedback formation scenario over predicts the sizes of isolated dwarf galaxies and cannot explain the relative abundances of cluster and field UDGs. Working with simulations of dwarf galaxies in clusters, Carleton et al. (2019) found that tidal stripping of dwarf galaxies with cored haloes is better than cuspy haloes in reproducing the observed UDG population. Specifically, they found that progenitors with cored haloes better reproduce the observed stellar mass, size and metallicity distributions. They found in their simulations that the abundance of tidally stripped UDGS increases with host cluster mass and found good agreement with the observed abundances. However, their models fail to reproduce extremely large UDGs, and galaxies that experience more than 99% mass loss.

In favor of an ex-situ origin, the work by (van der Burg et al., 2017) using the spectrographic GAMA survey to study 325 groups of galaxies, found that the abundances of UDGs in groups or clusters increases with the mass of the host. They further found the size distribution of UDGs to be very steep such that larger UDGs are rare. We focus on the globular cluster (GC) formation on Ultra diffuse galaxies as they have been found to be peculiar. The ex-situ hypothesis predicts top-heavy GC mass functions from simulations (Carleton et al., 2021) and the observation of luminous GC in UDGs like NGC1052-DF2 , DF4 and DGSAT I, which lead to top-heavy globular cluster luminosity function (GCLF) for UDGs in

groups (DF2 and DF4) and isolation (DGSAT I). We aim to study the GCLFs of UDGs as a whole but always considering the environment of the UDGs (cluster, group or isolation). In Chapter 2, we present our methodology for identifying the dominant UDG formation mechanisms operating in both isolated and cluster environments. In Chapter 3, we present our result for the different environments, such as if it is a in-situ mechanism or a ex-situ mechanism which predominates in each environment.

Chapter 2

Methods

We use publicly available catalogs of GCs in UDGs, taking the properties of their host galaxies reported in the literature, such as effective radius, stellar mass, Sérsic index and mean surface brightness in the F814W filter to perform our analysis on the GC populations. These parameters are listed in Table **??**. All the other parameters are derived or estimated as explained in the subsequent sub-sections. In Section 2.1 we show skewed gaussian fits to the GCLFs of the UDGs. In Section 2.3, we calculate the radial profiles for mass, density and velocity dispersion by fitting observable parameters to the appropriate theoretical functions. In Section 2.2 we estimate the effective mass-to-light ratio using a function dependent on log σ and log I_e (see Zaritsky and Behroozi 2022). Finally, in sections 2.4 and 2.5 we calculate dynamical friction (DF) and disruption timescales for all GCs reported in each UDG.

2.1 Globular cluster luminosity functions

First, we need to estimate how the magnitude errors from the observations affect our GCLF histograms due to the binning process. We use a bin size of 0.5 mag for all GCLFs. GCs falling near the edge of the bins have the possibility of being in one bin or another due to uncertainties in their magnitudes. In order to account for this uncertainty in our fitting procedure we first do a bootstrapping of 10000 subsamples created from the original GC magnitudes while folding in their observational uncertainties. We then create histograms for each and using the bin heights standard deviations, meaning how much the height of each bar in

the histogram changes across the ten thousand subsamples, from the subsamples as the errors for the bins of the original sample.

We fit a Gaussian and a Skew-Gaussian function to the GCLFs. The GCLF has been historically approximated by a Gaussian function (Secker and Harris 1993) described by its mean (μ_g) or turnover magnitude (M_0^T) and it's standard deviation (σ_g). To account for how the GCLFs may have been shaped by different dynamical processes affecting GCs we also fit a Skew-Gaussian function. For the turnover magnitude we use the mode, standard deviation (just as in a Gaussian) and the third parameter is skewness which measures its asymmetry. For the Gaussian $g(x, \mu_g, \sigma_g)$ we use:

$$g(x, \mu_g, \sigma_g) = \frac{1}{\sqrt{2\pi}\sigma_g} \cdot \exp\left(-\frac{(x-\mu_g)^2}{2\sigma_g^2}\right) \tag{2.1.1}$$

For the Skew-Gaussian function $s(x, \xi, \omega, \alpha)$ we fit the location (ξ), scale (ω) and shape (α) parameters. We then calculate the turnover magnitude($M_{0,skew}^T$), standard deviation (σ_s) and skewness(γ_1).

$$s(x, \xi, \omega, \alpha) = \frac{2}{\omega}\phi\left(\frac{x-\xi}{\omega}\right) \cdot \Phi\left(\alpha\left(\frac{x-\xi}{\omega}\right)\right) \tag{2.1.2}$$

Where ϕ and Φ are the normal probability density function and cumulative density function, respectively.

In order to properly fit those parameters we take advantage of the non-linear least squares algorithm implemented in *curvefit* from the *Python* package *SciPy* (Virtanen et al. 2020).

2.2 Mass to light ratio estimation

In order to calculate various theoretical quantities we need mass-to-light relations. We estimate mass-to-light ratios using the ansatz in the form of $\Upsilon_e = f(\log\sigma, \log I_e)$ proposed by Zaritsky and Behroozi 2022, with parameters $a = 0.198$, $b = 0.140$, $c = 0.192$, $d = -0.923$, $e = -0.108$, and $f = 1.306$. These parameters were obtained through fitting elliptical and dwarf elliptical galaxies, ultra-diffuse galaxies (UDGs), dwarf spheroidal and ultra-faint satellites of the Milky Way and M31, as well as compact dwarf galaxies.

$$\log \Upsilon_{\rm e} = a\,(\log \sigma)^2 + b \log \sigma + c\,(\log I_{\rm e})^2 + d \log I_{\rm e} + e \log I_{\rm e} \log \sigma + f \quad (2.2.1)$$

For NGC1052-DF2, NGC1052-DF4 and DGSAT-I the velocity dispersion has been measured (van Dokkum et al. 2018a, Shen et al. 2023 and Janssens et al. 2022 respectively). For the UDGs in the Coma cluster we estimate velocity dispersions in order to study at the order of magnitude level the dynamical properties of the GC populations. We re-arrange equation (3) in Zaritsky and Behroozi 2022 to obtain a function that relates σ, r_e and I_e (see table 2.2.1 for r_e and I_e).

$$f(\sigma, r_e, I_e) = 2\log \sigma - \log I_e - \log r_e - \log \Upsilon_e(\sigma, I_e) - 0.53 \quad (2.2.2)$$

Our estimation of velocity dispersion is therefore the root of this equation, which is unique in the desired range $0 - 200$ km/s. With the estimation of velocity dispersion and mass to light ratio we proceed into calculating the radial profiles of the UDGs.

2.3 Mass, density and velocity dispersion

To calculate the DF timescales for all GCs in our UDGs, we first need to compute numerically the mass, density, and velocity dispersion profiles. The mass enclosed within a radius r is required to calculate the density and velocity dispersion profiles. This is done by fitting observational parameters such as the Sérsic index, n, and the central intensity, I_0. Following Leigh and Fragione (2020), we use equation (A2) from Terzić and Graham (2005), which corresponds to the enclosed mass M(r):

$$M(r) = 4\pi\rho_0 R_{\rm e}^3 n b^{n(p-3)} \gamma(n(3-p), z) \quad (2.3.1)$$

where $\gamma(a, x)$ is the incomplete gamma function and z is a dimensionless variable defined as $z = b\left(\frac{r}{R_e}\right)^{1/n}$. Also, ρ_0 is a normalization factor with units of density ($[M_\odot/pc^3]$) that makes the total mass from the density profile equal to the enclosed

Table 2.2.1

Galaxy	R_e [kpc]	I_e [$L_\odot/pc^2$]	n	refs.
DF2	1.40	4.50	0.60	(a),(b)
DF4	1.20	4.32	0.86	(c),(d)
DF2*	2.20	4.03	0.55	(d),(e)
DF4*	1.70	4.75	0.79	(d),(f)
DF07	3.55	3.35	0.81	(g)
DF08	2.95	1.44	0.88	(g)
DF17	3.45	1.85	0.65	(g)
DF44	3.92	2.35	0.77	(g)
DFX1	3.69	2.31	0.92	(g)
SMDG1251014	4.99	2.10	1.01	(g)
DGSAT-I	4.00	2.45	0.38	(h)

Note. Column (1) is the name of each UDG, column (2) is the effective radius in kpc, column (3) the surface brightness within R_e in units of solar luminosities per squared parsec and column (4) is the Sérsic index of each UDG. Refs: (a) (Montes et al., 2021), (b) Trujillo et al. (2019), (c) Montes et al. (2020),(d)Shen et al. (2021),(e) van Dokkum et al. (2018b),(f) van Dokkum et al. (2019), (g) Saifollahi et al. (2022) and (h) Janssens et al. (2022)

* assuming a distance of $\sim$ 20 Mpc instead of $\sim$ 13 Mpc

mass.

$$\rho_0 = \Upsilon_0 I_0 b^{n(1-p)} \frac{\Gamma(2n)}{2R_e\Gamma(n(3-p))} \tag{2.3.2}$$

where Υ_0 is the mass-to-light ratio. The b and p depend only on the Sérsic index n and can be approximated as:

$$b = 1.9992n - 0.3271 \tag{2.3.3}$$

$$p = 1 - \frac{0.6097}{n} + \frac{0.055}{n^2} \tag{2.3.4}$$

For the density profile, we use the three-parameter (ρ_0, R_e, n) density profile of Prugniel and Simien (1997):

$$\rho(r) = \rho_0 \left(\frac{r}{R_e}\right)^{-p} e^{-b(r/R_e)^{1/n}}, \tag{2.3.5}$$

Finally, the spatial velocity dispersion profile follows equation (A5) from Terzić

and Graham (2005) which is the numerical solution of:

$$\sigma^2(r) = \frac{G}{\rho(r)} \int_r^\infty \rho(\bar{r}) \frac{M(\bar{r})}{\bar{r}^2} d\bar{r} \tag{2.3.6}$$

2.4 DF timescale

Following the approach of Leigh and Fragione (2020) for DF2 and DF4, we study the past collisional evolution of observed GC populations in our UDGs. We begin with the calculation of the DF (DF) timescales for each GC. DF is a process by which a moving object, such as a GC, loses momentum and kinetic energy via gravitational interactions with surrounding stars and dark matter. The stars and/or DM end up being gravitationally focused into a trailing over-density, pulling back on the moving GC and reducing its velocity. This results in the object gradually spiraling inward towards the center of its host galaxy.

DF timescales shorter than a Hubble time suggest formation scenarios in which the GC populations have had enough time for their orbits to become more centrally concentrated. This is a key aspect of understanding the dynamical history and evolution of GCs within their host galaxies. Tremaine et al. (1975) proposed that nuclear star clusters (NSCs) could be formed by the sink of massive GCs due to DF. This process has been supported by observational and analytic works on low-mass early-type galaxies and has likely been a key process increasing the mass budget in NSCs (Neumayer et al. 2020).

Comparing the DF timescales with a Hubble time will provide valuable information about how much their initial positions must have changed over time. In cases where the DF timescales are shorter than a Hubble time, we expect that the GCs will have migrated inward, meaning their current locations are not where they originally formed. This information helps us to reconstruct the formation and evolutionary history of the GC populations in their host galaxies.

The DF timescale ($t_{\rm DF}$) assuming circular orbits is given by (Binney and Tremaine, 1987; Gnedin et al., 2014):

$$t_{\rm DF} = \frac{1.17\, M(r)\, r}{\ln \Lambda\, m_{\rm GC}\, \sigma(r)} \tag{2.4.1}$$

The GCs more affected by DF are those more massive and centrally located in the galaxy. Hence, as GCs migrate deeper in the potential, the DF rate increases.

2.5 Disruption timescale

As DF primarily affects high mass GCs and thus the high luminosity end of the GCLF, we use the disruption timescale to constrain the past evolution of the low mass (i.e low luminosity) end of the GCLF. We predict a lack of low-mass GCs, especially in the more dense regions of the UDGs. As their disruption timescales will be significantly less than a Hubble time.

To calculate disruption timescales we use equation (8) from Lamers et al. (2005)

$$t_{\rm dis} \simeq 810 \left(\frac{M_{cl}}{10^4\, M_\odot} \right) \rho_{\rm amb}^{-1/2} \ {\rm Myr} \tag{2.5.1}$$

We expect that any GC of low mass ($< \sim 10^5$ $M_\odot$) has already disrupted, further narrowing the GCLF of UDGs.

Chapter 3

Results

In this section we present our results for the analysis explained in the method section 2. In subsection 3.1 the fits to GCLFs are shown along with the statistical analysis of the retrieved parameters. Subsection 3.2 shows our study on the spatial distribution of the GCs populations. In subsection 3.3 we present results from our work estimating mass-to-light ratios along with our calculation of density, mass and velocity profiles. Subsection 3.4 and 3.5 present our calculations of timescales, DF and disruption respectively, for each GC in the UDGs.

3.1 Globular cluster luminosity function

We present our fits for the GCLFs of 9 UDGs using both a gaussian function and a skew-gaussian function (2.1). Figure 3.1.1 presents the fits and table 3.1.1 the fitted parameters for both distributions along with the number of GCs used for each UDG.

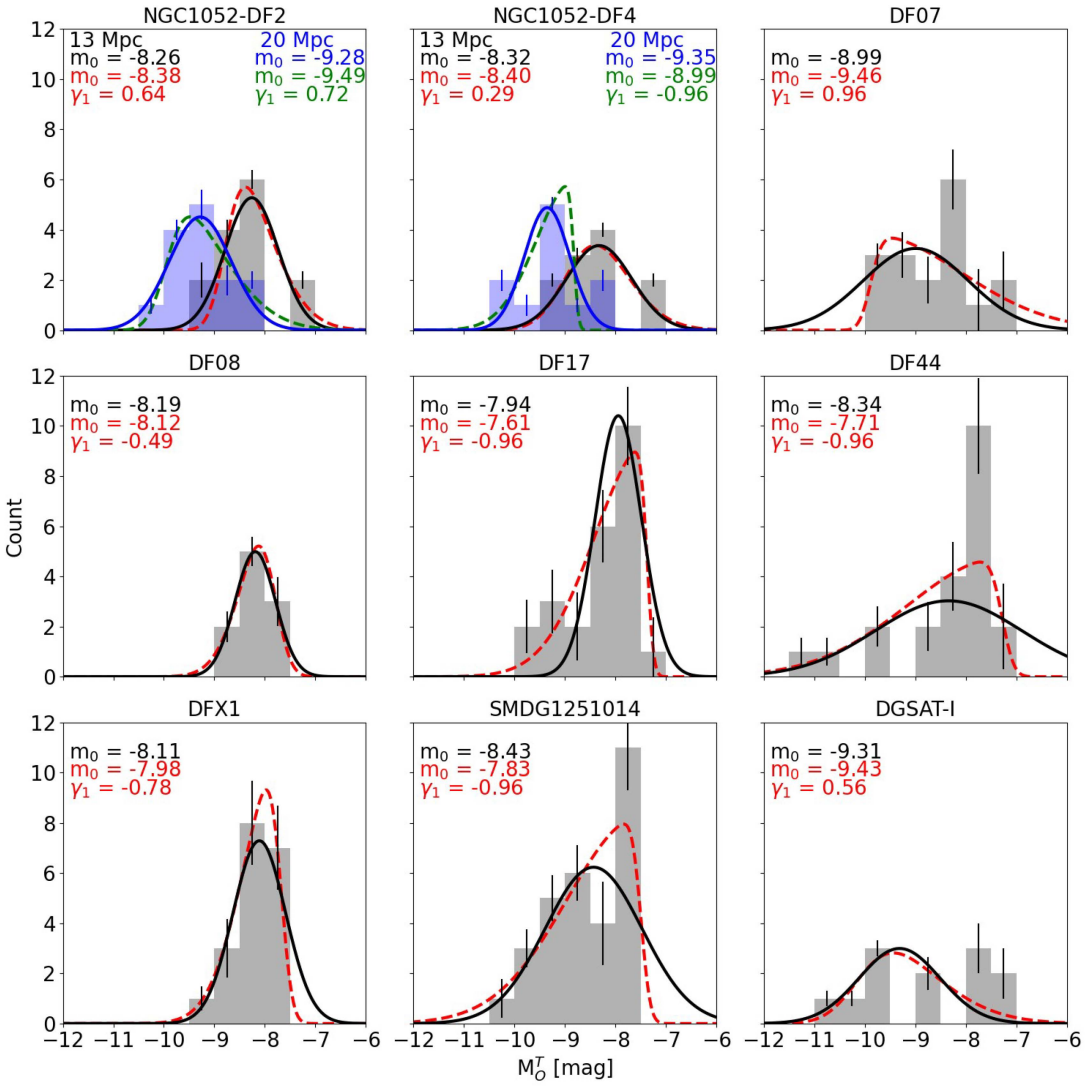

Figure 3.1.1: Gaussian and Skew-gaussian GCLFs for the UDGs in our sample. Black solid lines are the gaussian fits and red dashed lines are the skew-gaussian fits. In the case of DF2 and DF4 blue and green are the fits, gaussian and skew-gaussian respectively, for a distance of 20 Mpc

For the case of those two peculiar UDGs in NGC1052, namely DF2 and DF4, (see van Dokkum et al. 2018a, Trujillo et al. 2019, Shen et al. 2021, Montes et al. 2021 and Montes et al. 2020) we present fits to their GCLF at 20 Mpc and 13 Mpc.

Galaxy	N_{GC}	Gaussian		Skew-Gaussian		
		M_0^T	σ	$M_{0,skew}^T$	σ	γ_1
DF2	14	-8.26 ± 0.11	0.53 ± 0.12	-8.38 ± 0.20	0.53 ± 0.11	0.64
DF4	11	-8.32 ± 0.10	0.65 ± 0.10	-8.40 ± 0.10	0.66 ± 0.10	0.29
DF2*	14	-9.28 ± 0.11	0.62 ± 0.13	-9.49 ± 0.11	0.68 ± 0.14	0.72
DF4*	11	-9.35 ± 0.11	0.45 ± 0.12	-8.99 ± 0.16	0.45 ± 0.15	-0.96
DF07	17	-8.99 ± 0.16	1.04 ± 0.18	-9.46 ± 0.26	1.08 ± 0.20	0.96
DF08	10	-8.19 ± 0.15	0.40 ± 0.13	-8.12 ± 0.31	0.40 ± 0.14	-0.49
DF17	24	-7.94 ± 0.14	0.46 ± 0.18	-7.61 ± 0.17	0.62 ± 0.17	-0.96
DF44	22	-8.34 ± 0.15	1.45 ± 0.20	-7.71 ± 0.24	1.13 ± 0.20	-0.96
DFX1	19	-8.11 ± 0.15	0.52 ± 0.15	-7.98 ± 0.27	0.45 ± 0.16	-0.78
SMDG1251014	30	-8.43 ± 0.13	0.96 ± 0.13	-7.83 ± 0.39	0.88 ± 0.14	-0.96
DGSAT-I	12	-9.31 ± 0.29	0.80 ± 0.15	-9.43 ± 0.67	0.90 ± 0.24	0.56

Table 3.1.1: Fitted parameters for the GCLFs of UDGs in the sample, * are the fitted parameters considering a distance of 20 Mpc instead of 13 Mpc

Our Gaussian fits are consistent with those previously done for the UDGs in the sample. Skew Gaussian fits, on the other hand, are also consistent in turnover magnitudes with Gaussian peaks, except in cases where the absolute value of skewness is greater than ~ 0.5. The other cases are $\gamma_1 < -0.5$ where the Gaussian peak is brighter than the skew Gaussian peak and $\gamma_1 > 0.5$ where the Gaussian peak is fainter than the skew Gaussian peak. We interpret this as either an excess of low-mass GCs or a lack of high-mass GCs.

We perform Kolmogorov-Smirnov (KS) tests between the Gaussian and skew Gaussian parameters of our sample and the GCLF parameters of dwarf galaxies in the ACS Virgo and Fornax cluster survey (Villegas et al. 2010) to assess if the distribution of the GCLF parameters of UDGs is statistically different from that of "normal" galaxies in the same mass range. Three null hypothesis are tested; (i) the two cumulative distribution functions (CDF) are equal F(x)=G(x) for all x, (ii) F(x) $\geq$ G(x) for all x and (iii) F(x) $\leq$ G(x) for all x. With x representing each of the fitted values in the KS test (i.e. peak magnitude and standard deviation). The results from the KS test are presented in Table 3.1.2

Null Hypothesis		**F(x)=G(x)**		**F(x)≤G(x)**		**F(x)≥G(x)**	
		statistic	p-value	statistic	p-value	statistic	p-value
Gaussian	M_0^T	0.284	0.429	0.284	0.216	0.016	0.982
	σ	0.442	0.053	0.442	0.027	0.079	0.862
Skew gaussian	M_0^T	0.214	0.763	0.214	0.405	0.190	0.488
	σ	0.425	0.069	0.425	0.034	0.016	0.981

Table 3.1.2: KS test results of the three hypotheses tested when comparing the GCLF parameters of our sample with those of "normal" dwarf galaxies from Villegas et al. (2010). We reject the hypothesis when p-value < 0.05.

For both fits (gaussian and skew-gaussian) to the UDGs GCLFs we can reject the null hypothesis $F(x) \leq G(x)$ for the standard distribution in favor of the alternative $F(x) > G(x)$, where $F(x)$ would be the CDF of the standard deviations of the UDGs GCLF and $G(x)$ for the "normal" dwarf galaxies. This can be interpreted as the GCLF of UDGs being in trend narrower (i.e. smaller σ) than the GCLF of "normal" dwarf galaxies.

3.2 Globular cluster spatial distributions

We also study how the GCs are spatially distributed in each UDG. There is an increasing trend of UDGs having GC half number radius smaller than their effective radius (Janssens et al. 2022). Tidal forces from massive galaxies and disruption could strip/destroy GCs from the outskirts making a centrally concentrated distribution. Especially massive GCs experiencing DF will sink into the galaxy center, further enhancing the centrally concentrated distribution.

We focus especially on the spatial disruption and how this has been affected by DF and disruption processes.

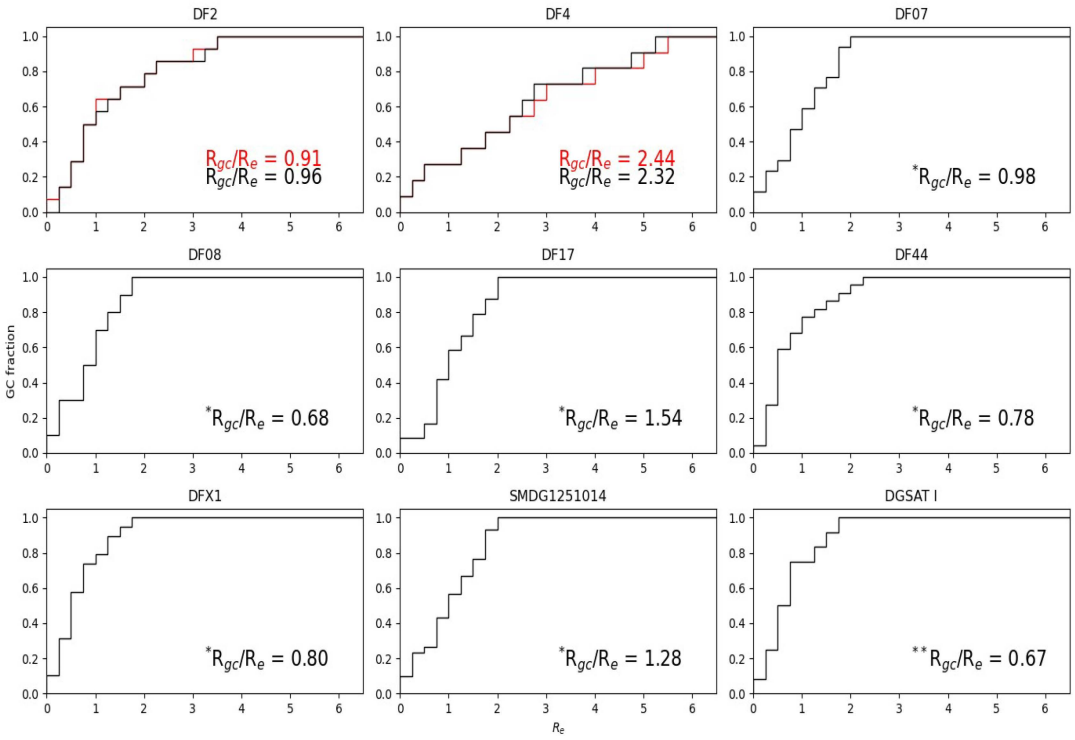

Figure 3.2.1: Cumulative density histogram of GC spatial distributions in their respective UDGs normalized by their effective radius. For DF2 and DF4 we test two different hypotheses for the distance, 13 and 20 Mpc respectively * from Saifollahi et al. 2022 and ** from Janssens et al. 2022

The only UDG without $R_{gc}/R_e < 2$ is NGC1052-DF4. Montes et al. (2020) shows NGC1052-DF4 is ongoing tidal disruption by its neighboring galaxy NGC1035. This interaction is affecting at first the DM. The GCs alignment with the orbit suggest they are also being stripped. This could be the main cause of the large R_{gc}/R_e of NGC1052-DF4 as we see in fig 3.2.1 and Fig 3.2.2 where we stacked Coma UDGs to better compare the distributions.

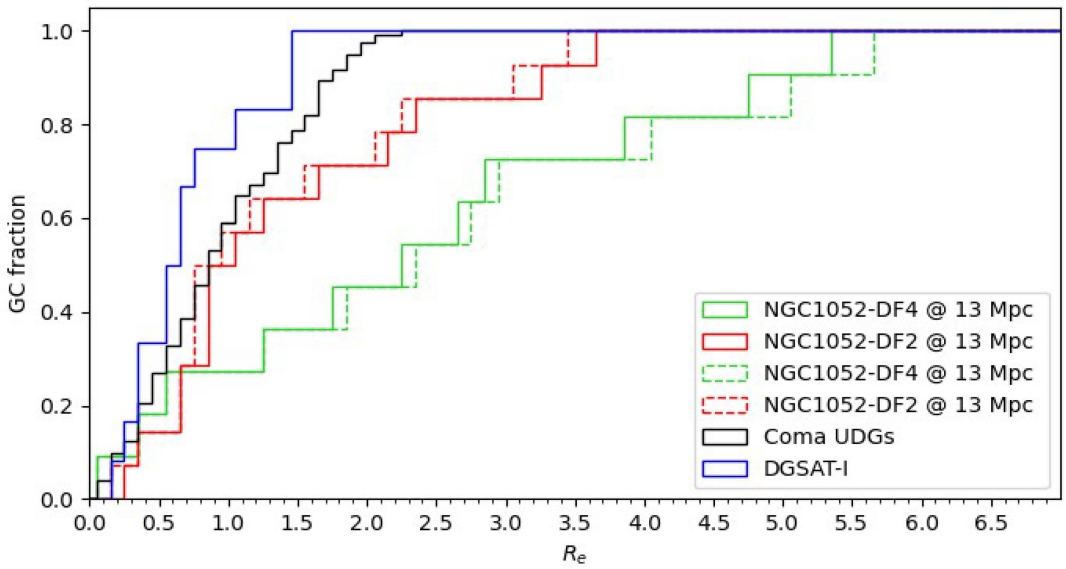

Figure 3.2.2: Cumulative density histograms of the GC spatial distributions. The difference in spatial distribution of NGC1052-DF4 (red histogram) is clear. We group those in Coma together to avoid over-plotting. Color code follows the legend in lower right.

3.3 Estimation of radial profiles

Using the equations presented in section 2 we estimate mass to light ratios (see 2.2) and calculated radial profiles of enclosed mass, density and velocity dispersion (see 2.3) for the UDGs in our sample. Here we present results from those calculations in table 3.3.1 and we plot the respective profiles in Fig 3.3.1. These profiles will be later used to calculate DF and disruption timescales for each GC in their host galaxy.

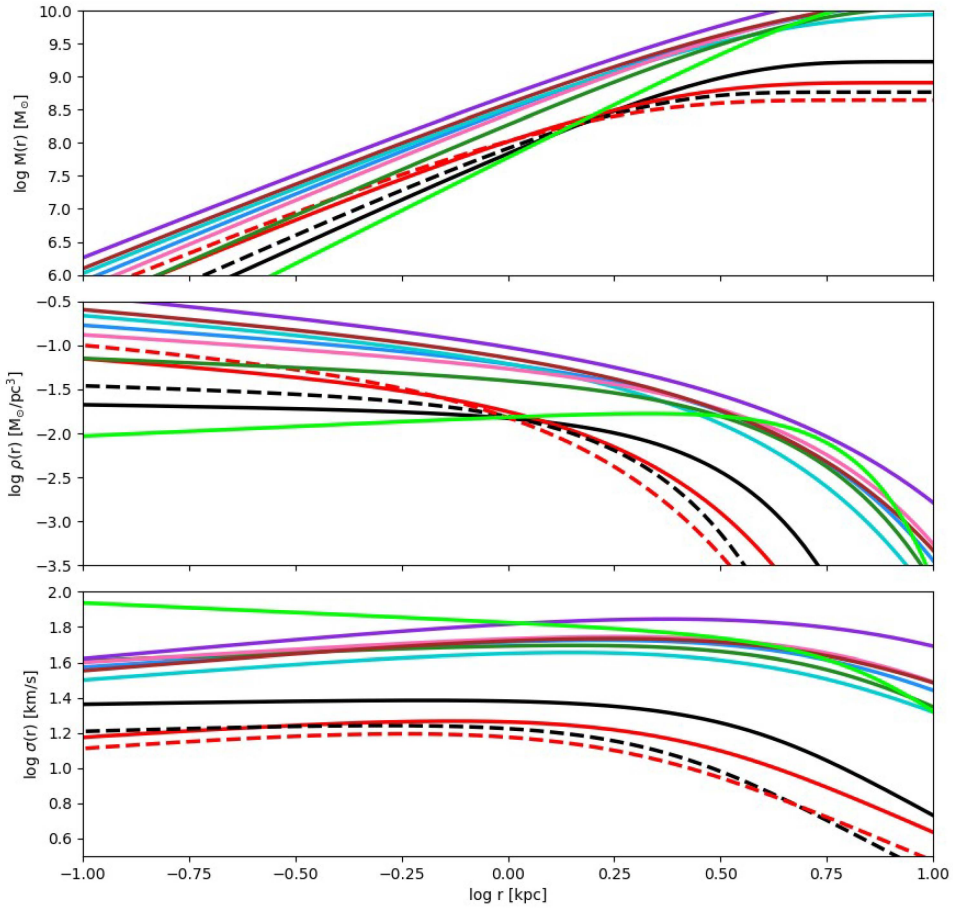

Figure 3.3.1: Top figure is the enclosed mass profile following equation 2.3.1. Middle figure is the density profile, equation 2.3.5. Finally, bottom figure is the velocity dispersion profile from equation 2.3.6. Color code for each UDG is: DF2: black (dashed line 13 Mpc; solid line 20 Mpc), DF4: red (dashed line 13 Mpc; solid line 20 Mpc), DF07: blue, DF08: turquoise, DF17: green, DF44: pink, DFX1: brown, SMDG1251014: violet and DGSAT-I: lime

Galaxy	M(r_e) [$M_\odot$]	$\rho(r_e)$ [$M_\odot/pc^3$]	$\sigma(r_e)$ [km/s]	Υ_e [$M_\odot/L_\odot$]
DF2	1.73×10^8	0.0102	15.596	10.48
DF4	1.44×10^8	0.0108	14.430	9.97
DF2*	4.87×10^8	0.0078	21.238	11.44
DF4*	2.59×10^8	0.0087	17.003	9.27
DF07	4.79×10^9	0.0144	48.857	29.54
DF08	2.97×10^8	0.0149	41.693	58.76
DF17	3.63×10^9	0.0136	44.841	49.84
DF44	5.67×10^9	0.0131	51.032	42.49
DFX1	5.44×10^9	0.0135	50.088	41.74
SMDG1251014	1.26×10^{10}	0.0120	64.652	54.55
DGSAT-I	4.14×10^9	0.0136	50.223	56.46

Table 3.3.1: Column (2) is the enclosed mass at r_e, column (3) is the density at r_e, column (4) is the spatial velocity dispersion at r_e and column (5) is the estimated mass-to-light ratio.

* assuming a distance of 20 Mpc instead of 13 Mpc

3.4 DF timescales

To create a profile for DF timescales we use two test GCs of masses 10^6 and 10^4 $M_\odot$ and calculate DF as a function of r. Figure 3.4.1 shows that, for our test GC mass of 10^6 $M_\odot$, the DF timescale becomes increasingly important in the inner $\sim$ 3 kpc. As for GCs of mass 10^4 $M_\odot$ it becomes relevant in the innermost regions of the UDGs (<0.5 kpc).

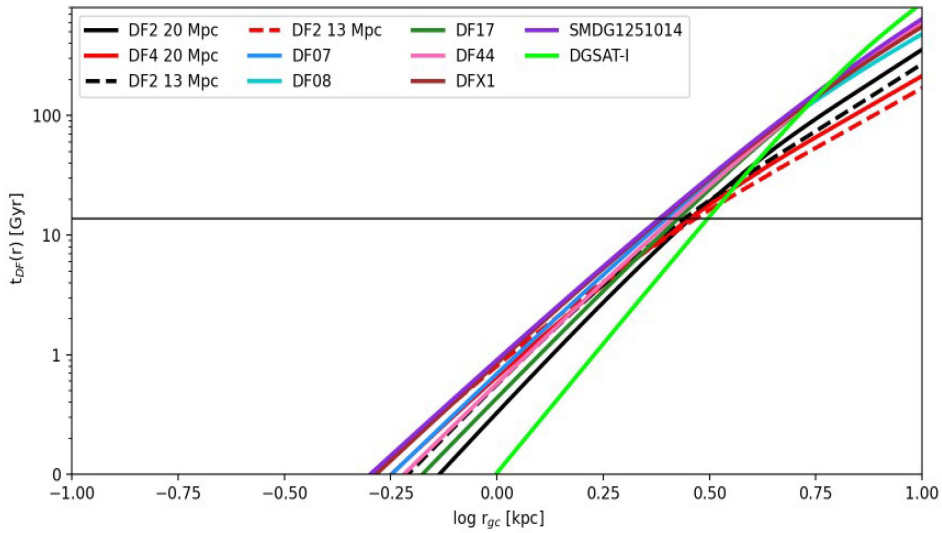

Figure 3.4.1: DF radial profiles for each UDG in the sample using a test GC mass of 10^6 $M_\odot$. The black horizontal line correspond to a Hubble time $\sim$ 13.7 Gyr Color code for each UDG is: DF2: black, DF4: red, DF07: blue, DF08: turquoise, DF17: green, DF44: pink, DFX1: brown, SMDG1251014: violet and DGSAT-I: lime

Using equation 2.4.1 and the previously presented profiles (see 3.3) we calculate DF timescales (t_{df}) for each GC in our UDGs. The results are presented in Fig 3.4.2. Each GC mass was derived assuming a mass-to-light ratio of 2 $M_\odot/L_\odot$. The number of GCs for which t_{df} was calculated is presented in table 3.1.1.

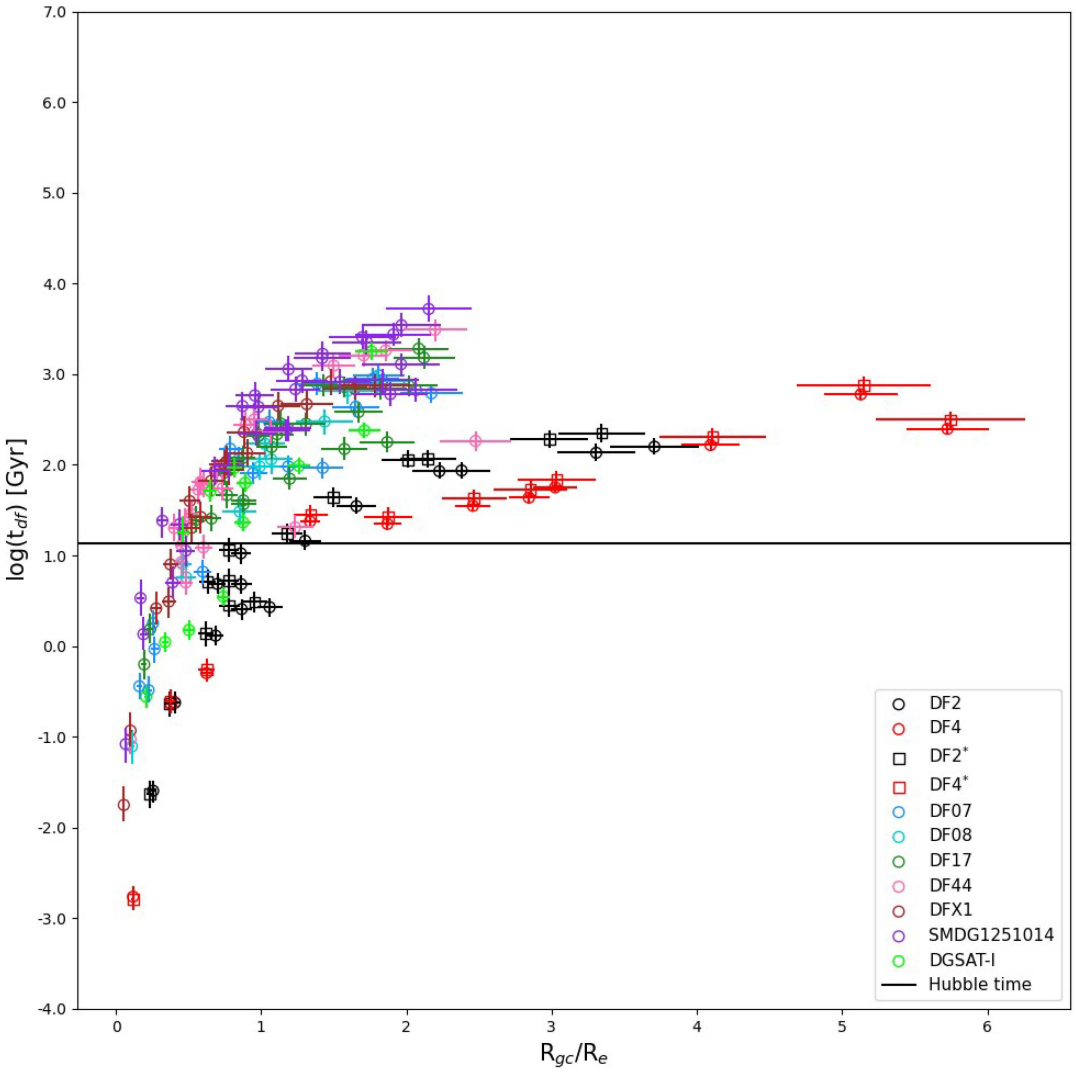

Figure 3.4.2: DF timescales for each GC in the UDGs as a function of their galactocentric radius normalized by the effective radius of each host galaxy. The black horizontal line represents a Hubble time $\sim$ 13.7 Gyr. Color code for each UDG is: DF2: black (dashed line 13 Mpc; solid line 20 Mpc), DF4: red (dashed line 13 Mpc; solid line 20 Mpc), DF07: blue, DF08: turquoise, DF17: green, DF44: pink, DFX1: brown, SMDG1251014: violet and DGSAT-I: lime

* assuming a distance of 20 Mpc instead of 13 Mpc

As seen in Fig 3.4.2 several GCs, especially in the inner regions $R_{gc}/R_e<1$, have t_{df} timescales less than a Hubble time ($\sim$ 13.7 Gyr). We expect these GCs to have lost significant orbital energy, sinking deeper into their host galaxy's potential well.

Galaxy	$f_{df<H}$	$f_{r<R_e}$
DF2	0.57	0.50
DF4	0.27	0.27
DF2*	0.57	0.57
DF4*	0.27	0.27
DF07	0.29	0.47
DF08	0.30	0.50
DF17	0.08	0.42
DF44	0.23	0.68
DFX1	0.26	0.74
SMDG1251014	0.17	0.43
DGSAT-I	0.33	0.75

Table 3.4.1: t_{df} table.

* assuming a distance of 20 Mpc instead of 13 Mpc

In table 3.4.1 we present the fraction of GCs with t_{df} less than a hubble time ($f_{df<H}$) and the fraction of GCs with galactocentric radius less than the R_e of their host ($f_{r<R_e}$).

3.5 Disruption timescales

Using equation 2.5.1 and two test GCs of masses 10^6 and 10^4 $M_\odot$ we create radial profiles of disruption timescales. Test GCs of 10^6 $M_\odot$ shouldn't be affected by disruption effects at any radius, as shown by Fig 3.5.1. GCs of mass $\sim 10^4$ $M_\odot$ are more susceptible to disruption events within a Hubble time. This gives us a minimum limit for the GCLF around ~ -5.5 F814W (10^4 $M_\odot$) considering a M/L of 2 for the stellar populations of the GCs.

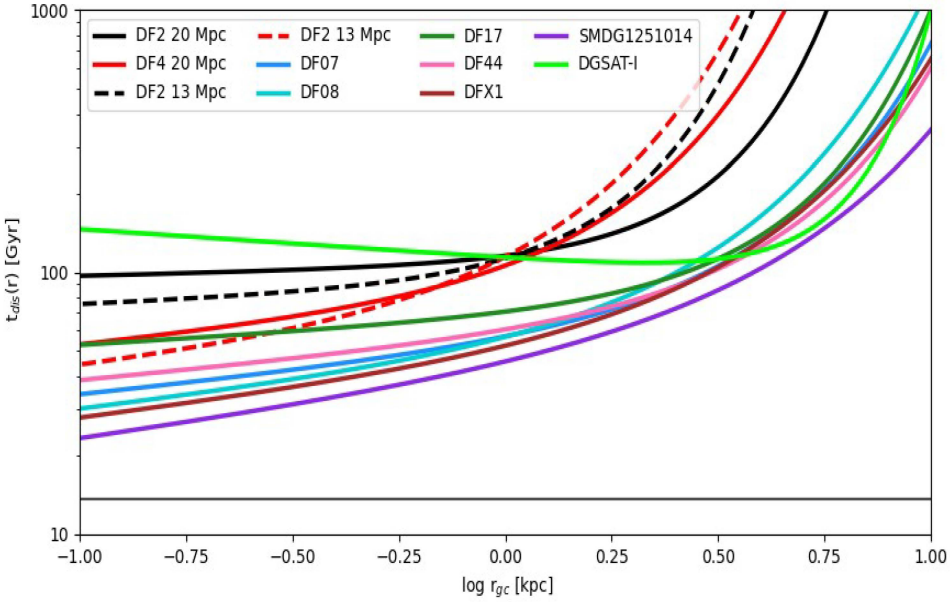

Figure 3.5.1: DF profiles for each UDG in the sample using a test GC mass of 10^6 $M_\odot$. The black horizontal line correspond to a Hubble time $\sim$ 13.7 Gyr. Color code for each UDG is: DF2: black (dashed line 13 Mpc; solid line 20 Mpc), DF4: red (dashed line 13 Mpc; solid line 20 Mpc), DF07: blue, DF08: turquoise, DF17: green, DF44: pink, DFX1: brown, SMDG1251014: violet and DGSAT-I: lime

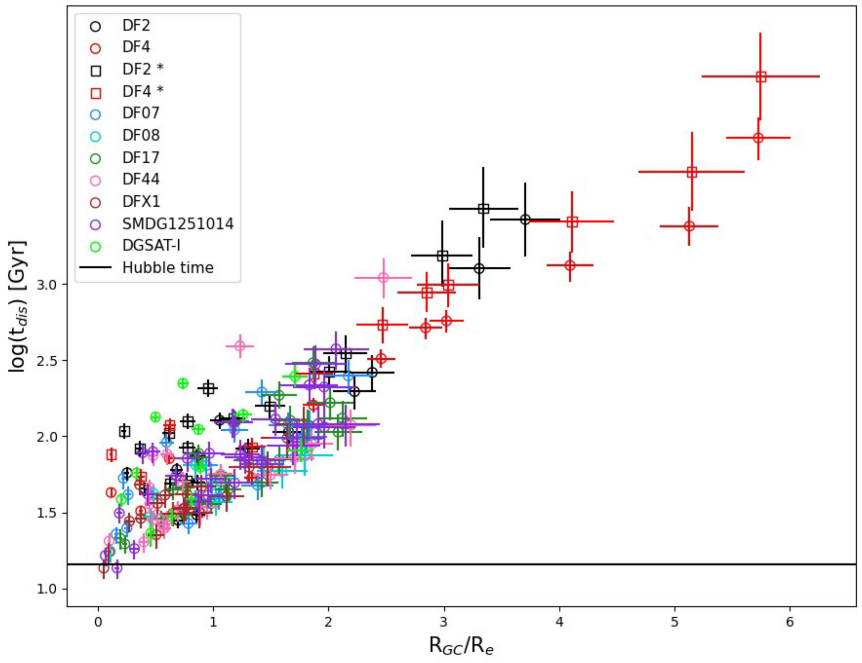

Figure 3.5.2: Disruption timescales for each GC in the UDGs. The black horizontal line represents a Hubble time $\sim$ 13.7 Gyr

We also calculate using equation 2.5.1 disruption timescales (t_{dis}) of each GC. As shown in Fig. 3.5.2.

3.6 Dynamical effects on GCs

In this subsection we combine our results of DF and disruption timescales, to study how both dynamical processes have shaped the GCs populations for each UDG. Fig. 3.6.1 shows those UDGs in Coma cluster. We calculated regions in the Mgc-Rgc parameter space where $t_{df} < t_h$ (grey shaded regions) and $t_{dis} < t_h$ (blue shaded regions).

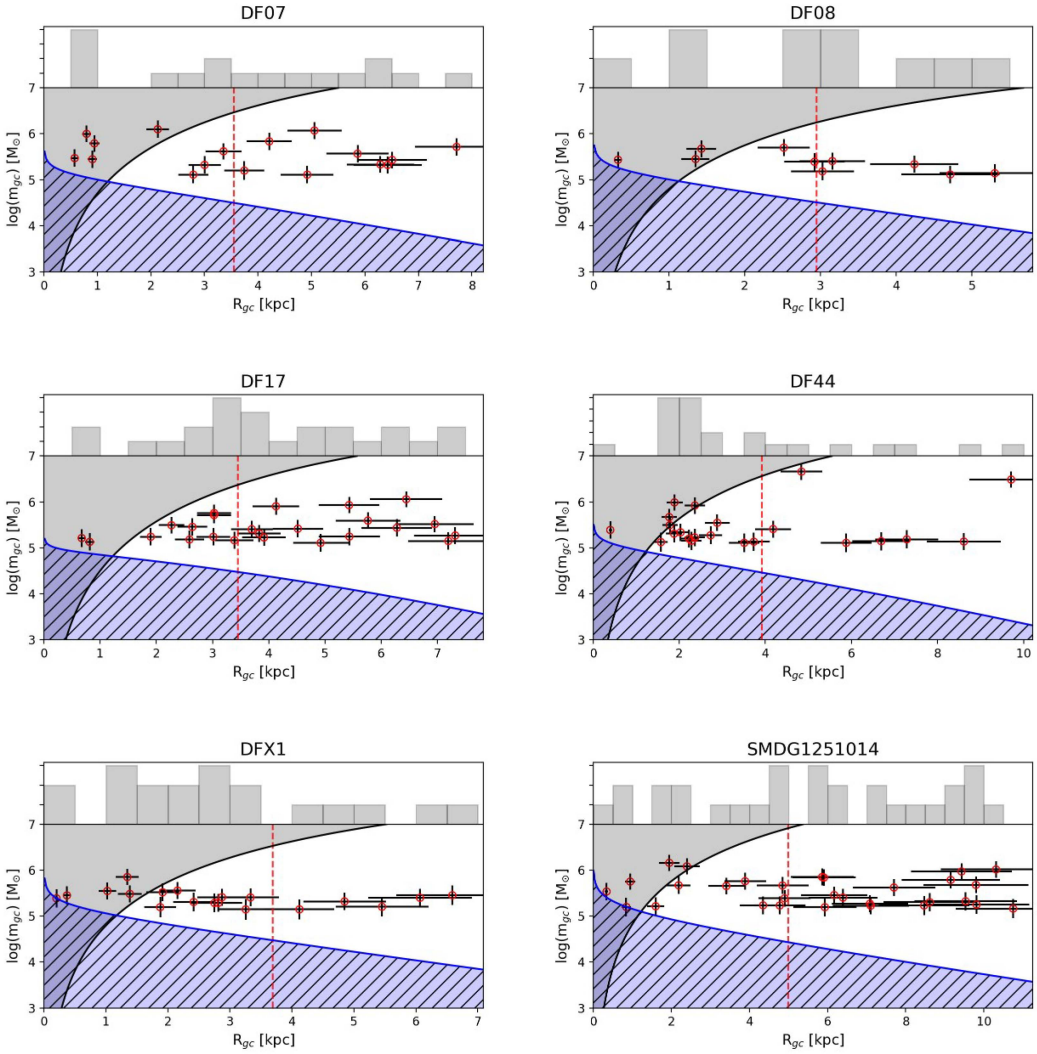

Figure 3.6.1: Radial distribution of GCs masses as a function of galactocentric distance for Coma UDGs. Grey and blue shaded regions represents $t_{df} < t_h$ and $t_{dis} < t_h$ respectively. Red dashed vertical line represent R_e

Fig. 3.6.2 is the same for UDGs DF2 and DF4 in NGC1052, we plot our results assuming both disntances 13 Mpc (Trujillo et al. (2019)) and 20 Mpc (van Dokkum et al. (2019); Shen et al. (2021)). For DF4 we added the tidal radius (r_{tidal}) as calculated by Montes et al. (2020).

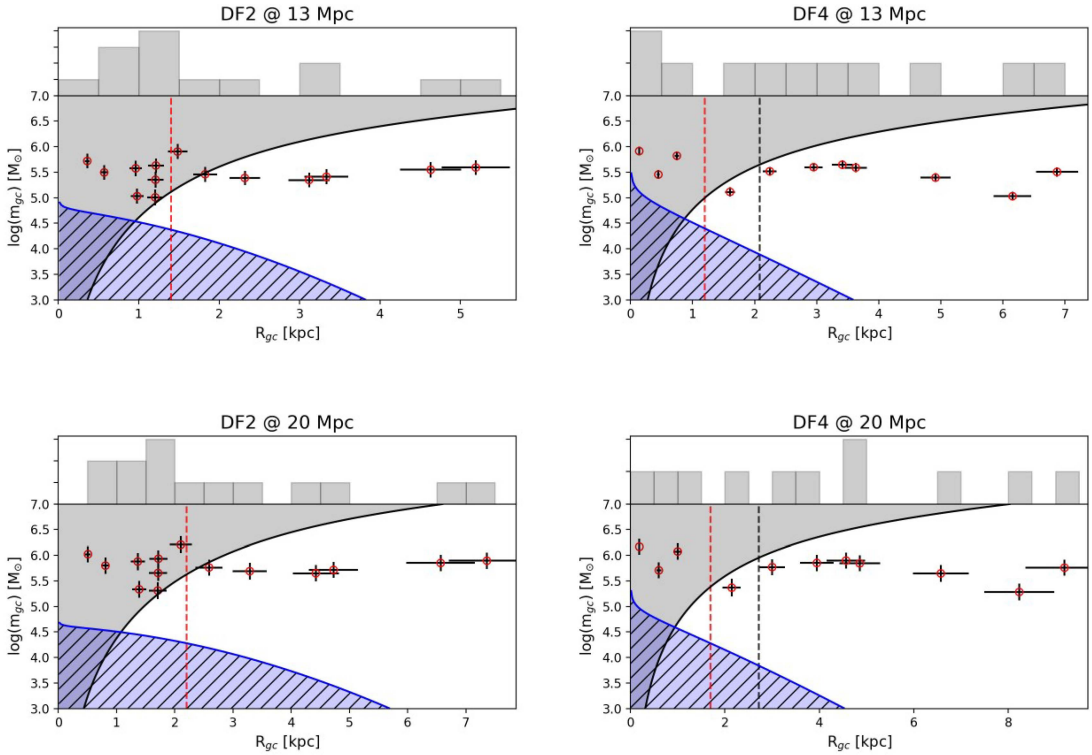

Figure 3.6.2: GC masses in solar units as a function of galactocentric distance in kpc for NGC1052 UDGs. Top rows are assuming a distance of 13 Mpc, bottom rows assuming 20 Mpc as distance. Black and blue shaded regions represent $t_{df} < t_h$ and $t_{dis} < t_h$, respectively. The red dashed vertical line represents R_e and the grey dashed line shows r_{tidal} for DF4 as calculated by Montes et al. (2020)

Finally Fig. 3.6.3 show our isolated UDG in the sample DGSAT-I.

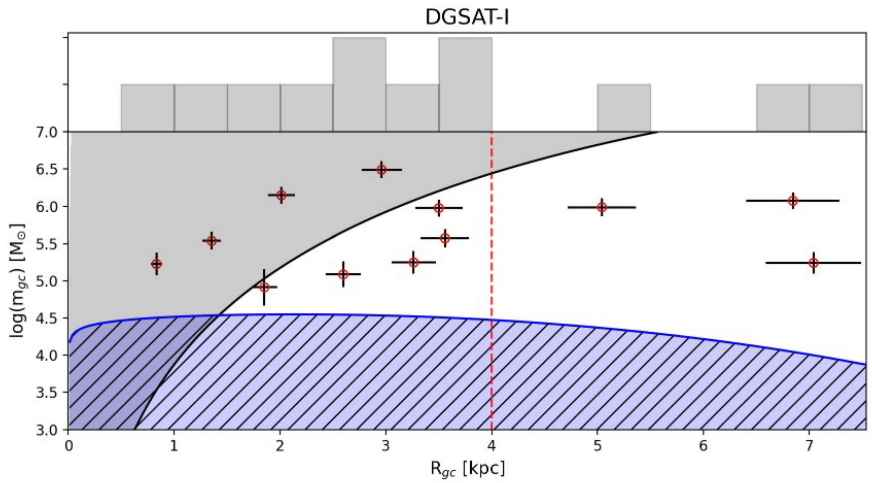

Figure 3.6.3: Radial distribution of GCs masses as a function of galactocentric distance for DGSAT-I. Black and blue shaded regions represents $t_{df} < t_h$ and $t_{dis} < t_h$ respectively. Red dashed vertical line represent R_e.

Chapter 4

Discussion

In this section, we will discuss our results for each individual galaxy or galaxy cluster and compare between them to address their formation histories.

4.0.1 Coma UDGs

The GCLFs of UDGs in the Coma cluster exhibit a smaller dispersion compared to those of typical dwarf galaxies Villegas et al. (2010). Skew Gaussian fits to the GCLFs (see fig. 3.1.1) reveal a tendency for negative skewness in all Coma UDGs except DF07, indicating an excess of low mass GCs. The tail extending towards massive GCs shows them as outliers that break the symmetry of the GCLF. DF07 shows positive skewness, indicating that the bulk of GCs are in the higher mass part of the distribution.

As seen in Figure 3.6.1, the disruption of low-mass GCs could have contributed to narrowing the GCLF. If there was an over abundance of high mass GCs we would expect a higher fraction of the stellar mass be in the form of GCs. DF07 has a relative low stellar mass fraction in GCs $M_{gc}/M_{*} = 0.28$.This leads us to believe is not an overabundance of high-mass GCs as a galaxy with such an effective GC formation would have convert a higher fraction of it's stellar mas into GCs.

Coma UDGs follow the general trend of R_{gc}/R_{e} observed in UDG systems (Janssens et al. 2022) with an average value of R_{gc}/R_{e} =1.01. This is noticeably lower than for dwarf galaxies ($R_{gc}/R_{e} \sim 1.5$, (Saifollahi et al., 2022)). Approximately half of the globular clusters in Coma UDGs are located within their effective radius

($f_{r<r_e} = 0.54$). The difference is a more centrally concentrated distribution of GCs for UDGs than for dwarf galaxies, along with the R_{gc}/R_e values.

The narrower GCLF and lower R_{gc}/R_e ratio in UDGs could suggest that dynamical processes play a significant, such as disruption of low-mass globular clusters and DF acting on preferntially massive GCs. These processes may explain the observed central spatial distribution (see Fig. 3.2.1) of GCs despite the high R_e characteristic of UDGs.

DF timescales for Coma UDGs indicate that on average a quarter ($f_{t_{df}<t_H}$=0.26) of their globular clusters have timescales shorter than a Hubble time. All GCs with $t_{df} < t_h$ are inside $1R_e$. This suggests that we may have caught them just before sinking deeper and forming an NSC Tremaine et al. (1975). Or the GCs are being stalled because of the decrease of DF effectiveness due to core stalling in a cored halo Read et al. (2006).

As seen in Fig. 3.6.1, in DF17 the most massive GCs are outside $1R_e$. It has a remarkably low fraction of GCs with $t_{df} < t_h$. The evidently low abundance of GCs in the inner most part of DF17 is intriguing. With DF timescales shorter than a Hubble time the formation of an NSC could explain the lack of GCs. However, DF17 shows no evidence of a central NSC most probably due to core stalling.

4.0.2 NGC1052 UDGs

In this subsection we will compare DF2 and DF4 taking into account both proposed distances, namely 13 Mpc (Trujillo et al. (2019); Montes et al. (2021, 2020)) and 20 Mpc (van Dokkum et al. (2018b, 2019); **?**). We also compare them with other UDGs and dwarf galaxies.

The GCLFs of DF2 and DF4 in the NGC1052 group exhibit a smaller $\sigma_{\rm gclf}$ than typical dwarf galaxies, with a mean $\sigma_{\rm gclf}$ of 0.59 assuming a distance d=13 Mpc or 0.54 assuming distance d=20 Mpc. Skew Gaussian fits reveal a tendency for positive skewness, indicative of a shift of the distribution towards high-mass globular clusters.

The spatial distribution of globular clusters differs significantly between DF2 and DF4. DF2 follows the typical $R_{gc}/R_e<1$ trend observed in UDGs, with values of 0.91 at 13 Mpc and 0.96 at 20 Mpc. Approximately half of its globular clusters

are located within 1 R_e ($f_{r<r_e} = 0.50$ and 0.57, assuming distances of 13 and 20 Mpc, respectively). In contrast, DF4 deviates substantially from this trend, with R_{gc}/R_e values of 2.32 at 13 Mpc and 2.44 at 20 Mpc.Montes et al. (2020) propose that DF4 is undergoing tidal disruption due to its interaction with NGC1035, affecting both its dark matter content and its globular cluster system. DF4 GCs outside r_{tidal} (7 of 11 GCs, see Fig. 3.6.2), the radius at which tidal effects become significant for DF4, are being pulled by NGC1035 explaining the large R_{gc}/R_e of DF4.

The dynamical processes that act on DF2 and DF4 are key to understanding their globular cluster systems. DF2 has the highest fraction of globular clusters with DF timescales shorter than a Hubble time in the sample, with $f_{df<H}$=0.57 at 13 Mpc and $f_{df<H}$=0.64 at 20 Mpc. As seen in Fig. 3.6.2, DF2 is heavily dominated by DF within it's Re. DF2 is the only UDG in the sample with GCs outside Re having $t_{df} < t_h$. This is mainly due to DF2 being less dense and therefore enclosing less mass as $t_{DF} \propto M(r)$.

4.0.3 DGSAT-I

DGSAT-I, the only isolated UDG in our sample, exhibits a GCLF with a bright peak magnitude and a dispersion ($\sigma = 0.8$) closer to that of dwarf galaxies. A skew Gaussian fit reveals a positive skewness of $\gamma_1 = 0.56$, suggesting of a higher relative abundance of high-mass globular clusters compared to low-mass ones.

The spatial distribution of globular clusters in DGSAT-I follows the general R_{gc}/R_e trend observed in UDGs, with R_{gc}/R_e=0.67 (Janssens et al., 2022). We expect this to be a primordial property of the UDGs as the low fraction of GCs with DF timescales lower than a Hubble time ($f_{df<H}$=0.33) suggests DF has not been the main mechanism concentrating the GCs inside R_e.

In contrast, the remaining globular clusters, with DF timescales exceeding a Hubble time, are expected to remain close to their original spatial distribution. This suggests that the current distribution of globular clusters outside R_e closely reflects the locations of their initial formation, assuming they are unaffected by significant external tidal forces.

4.0.4 Dynamical Timescales

Disruption timescales for the observed globular clusters are generally longer than a Hubble time, suggesting that the surviving clusters are resilient to tidal effects. However, analyzing the disruption timescales with test GC masses reveals a critical mass threshold of $\sim 10^{4.5}$ $M_\odot$ at all radii (see Fig. 3.6.3), below which the disruption timescales becomes shorter than a Hubble time. This could imply that low-mass GCs have been disrupted, narrowing down the GCLF of DGSAT-I.

When compared to dwarf galaxies, UDGs exhibit longer DF timescales but comparable disruption timescales. This indicates that while DF could be playing a significant role in shaping the globular cluster spatial distributions, the overall survival of clusters is governed by similar mechanisms working at similar timescales in both UDGs and dwarfs. This suggests disruption of low mass GCs is not responsible for narrowing down the GCLF of UDGs.

4.0.5 Why do we not see NSCs?

We calculate low DF timescales for several GCs inside R_e for our UDGs. None of the UDGs in our sample show evidence of having NSCs, which are supposedly formed by the sinking of GCs into the galaxy center due to DF Tremaine et al. (1975). This implies some process must be preventing the formation of the NSC or we are catching the UDGs just before this happens.

Lambert et al. (2024) found that UDGs have lower M_{NSC}/M_* than dwarf galaxies. This is consistent with our findings of UDGs having longer DF timescales than dwarf galaxies as the build up of NSC mass trough GCs sinking in the center would be slower and less efficient in UDGs. This suggests that the overall process of forming NSCs in UDGs is not as efficient as in dwarf galaxies.

Studying a heavily mass segregated UDG (NGC5846-UDG1), Bar et al. (2022) found that DF was able to explain the mass segregation of GCs, and the galaxy may be in an intermediate state where a nucleus has not yet been formed. Our galaxies may be in this intermediate state or even one step before as clear signals of mass segregation, a direct effect of DF, is yet to be observed.

Semi-analytical methods like ours and Bar et al. (2022) are in good agreement with simulations of cuspy galaxy haloes, where t_{df} decreases constantly as the

radius decreases. N-body simulations of GC orbits in a cored density profile (Read et al. (2006); Cole et al. (2012)) show that DF may be suppressed near the core radius and produce a stalling of GC infall, usually named as core stalling.

The lack of NSCs in our UDGs seems puzzling as we estimate DF timescales for the inner GCs several orders of magnitude shorter than a Hubble time. But this could be explained by UDGs having cored density profiles in which the effects of DF are suppressed due to the flattened density profile. This effect has not been evidenced in our method due to the rather cuspy profile of our model and the semi-analytic approach as discussed before.

Simulations of different formation scenarios for UDGs show a transition over time from cuspy to cored haloes. For example, Di Cintio et al. (2017) used zoom-in cosmological simulations and found UDG analogues formed by the expansion of dark matter and stellar content due to episodes of gas outlfow associated with star formation. These UDG analogues experienced a change in the inner slope γ of the DM halo from $\gamma \sim 1$ at z=4 to $\gamma = 0$ at z=0 (see Di Cintio et al. (2017) Fig. 3, panel d), denoting the transition from cuspy to cored halos in UDGs over time.

In cluster and group environments, Carleton et al. (2019) studied the effect of tidal stripping and heating on the stellar mass and half-light radius of dwarf satellites in cuspy and cored haloes. Their analysis found that tidally-stripped dwarf galaxies, residing in cored halos, are able to reproduce the observed sizes and stellar masses of UDGs in denser environments. Assuming that it is likely that there is no single formation mechanism responsible for the origins of all UDGs, it is most probable that a complex interplay of different mechanisms is at play. This suggests that the cored halo of UDGs could be a universal property of UDGs. Consequently, core stalling of GCs would be expected to occur in most, if not all UDGs. This is consistent with our results of low DF timescales and the lack NSC.

Because core stalling and dynamical buoyancy (Read et al. (2006); Cole et al. (2012)) are likely to occur in UDGs, we naively expect a low frequency of NSCs, which is consistent with what we observe. This result is consistent with the nucleation fraction of UDGs in the cores of clusters ($f_{nuc,\mathrm{UDG}} \approx 40\%$) being lower than the nucleation fraction of dwarf galaxies ($f_{nuc} \approx 60\%$). UDGs can decrease ths to $0\% - 20\%$ in the outskirts (Lim et al., 2018). Therefore, UDGs hosting NSCs likely formed them primordially.

Chapter 5

Conclusion

In this work we analyze the GC populations of UDGs, their luminosity function, spatial distribution and dynamical timescales. Through our analysis, we constrain the possible formation mechanisms for UDGs.

Our results are as follows.

1. Fits to the GCLFs of UDGs show that their peak luminosity is statistically consistent with dwarf galaxies, but a p-value=0.027 rejects the idea of their dispersion being consistent and favors UDGs having narrower GCLFs.

2. The emerging trend of UDGs having $R_{gc}/R_e < 1$ can't be completely explained by dynamical friction as most UDGs show a $f_{df<H}$ (fraction of GCs with t_{df} less than a Hubble time) significantly less than $f_{r<Re}$ (fraction of GCs inside Re).

3. Disruption timescales of GCs show the disruption of low-mass GCs could have contributed to narrowing the GCLFs at the low-mass end.

4. Dynamical friction timescales GCs in the inner regions of UDGs are well below a Huble time, yet we see no presence of NSCs. This is most likely due to effects of core stalling and dynamical buoyancy of GCs due to the cored density profile of UDGs. Hence, the high-mass end of the GCLF remains a mystery, since we do not observe NCSs in UDGs, suggesting that dynamical friction cannot explain a paucity of GCs at the high-mass end. Therefore, our results are consistent with these differences being primordial.

Our results are consistent with UDG formation models that redistribute the stellar content at higher radii reducing surface brightness and the resultant DM halo is cored (e.g stellar feedback, tidal heating and stripping.). The observed small R_{gc}/R_e is consistent with DF acting after any expansion process. Our analysis does not provide constraints in environment for the formation of UDGs, as we do not find significant differences between the UDGs in terms of their GC properties, including the one UDG in isolation (i.e., DGSAT-I) in different environments in how dynamical processes affects their GCs.

Bibliography

Amorisco, N. C. and Loeb, A. (2016). Ultradiffuse galaxies: the high-spin tail of the abundant dwarf galaxy population. , 459(1):L51–L55.

Bar, N., Danieli, S., and Blum, K. (2022). Dynamical friction in globular cluster-rich ultra-diffuse galaxies: The case of ngc5846-udg1. *The Astrophysical Journal Letters*, 932(1):L10.

Binney, J. and Tremaine, S. (1987). *Galactic dynamics*.

Carleton, T., Errani, R., Cooper, M., Kaplinghat, M., Peñarrubia, J., and Guo, Y. (2019). The formation of ultra-diffuse galaxies in cored dark matter haloes through tidal stripping and heating. , 485(1):382–395.

Carleton, T., Guo, Y., Munshi, F., Tremmel, M., and Wright, A. (2021). An excess of globular clusters in Ultra-Diffuse Galaxies formed through tidal heating. , 502(1):398–406.

Chan, T. K., Kereš, D., Wetzel, A., Hopkins, P. F., Faucher-Giguère, C.-A., El-Badry, K., Garrison-Kimmel, S., and Boylan-Kolchin, M. (2018). The origin of ultra diffuse galaxies: stellar feedback and quenching. *Monthly Notices of the Royal Astronomical Society*, 478(1):906–925.

Cole, D. R., Dehnen, W., Read, J. I., and Wilkinson, M. I. (2012). The mass distribution of the Fornax dSph: constraints from its globular cluster distribution. , 426(1):601–613.

Di Cintio, A., Brook, C. B., Dutton, A. A., Macciò, A. V., Obreja, A., and Dekel, A. (2017). Nihao–xi. formation of ultra-diffuse galaxies by outflows. *Monthly Notices of the Royal Astronomical Society: Letters*, 466(1):L1–L6.

Gnedin, O. Y., Ostriker, J. P., and Tremaine, S. (2014). Co-evolution of Galactic Nuclei and Globular Cluster Systems. , 785(1):71.

Janssens, S. R., Romanowsky, A. J., Abraham, R., Brodie, J. P., Couch, W. J., Forbes, D. A., Laine, S., Martínez-Delgado, D., and van Dokkum, P. G. (2022). The globular clusters and star formation history of the isolated, quiescent ultra-diffuse galaxy DGSAT I. , 517(1):858–871.

Koda, J., Yagi, M., Yamanoi, H., and Komiyama, Y. (2015). Approximately a Thousand Ultra-diffuse Galaxies in the Coma Cluster. , 807(1):L2.

Lambert, M., Khim, D. J., Zaritsky, D., and Donnerstein, R. (2024). Systematically Measuring Ultra-diffuse Galaxies (SMUDGes). VI. Nuclear Star Clusters. , 167(2):61.

Lamers, H. J. G. L. M., Gieles, M., and Portegies Zwart, S. F. (2005). Disruption time scales of star clusters in different galaxies. , 429:173–179.

Leigh, N. W. C. and Fragione, G. (2020). A New Method to Constrain the Origins of Dark-matter-free Galaxies and Their Unusual Globular Clusters. , 892(1):32.

Lim, S., Peng, E. W., Côté, P., Sales, L. V., den Brok, M., Blakeslee, J. P., and Guhathakurta, P. (2018). The globular cluster systems of ultra-diffuse galaxies in the coma cluster. *The Astrophysical Journal*, 862(1):82.

Mihos, J. C., Durrell, P. R., Ferrarese, L., Feldmeier, J. J., Côté, P., Peng, E. W., Harding, P., Liu, C., Gwyn, S., and Cuillandre, J.-C. (2015). Galaxies at the Extremes: Ultra-diffuse Galaxies in the Virgo Cluster. , 809(2):L21.

Montes, M., Infante-Sainz, R., Madrigal-Aguado, A., Román, J., Monelli, M., Borlaff, A. S., and Trujillo, I. (2020). The Galaxy "Missing Dark Matter" NGC 1052-DF4 is Undergoing Tidal Disruption. , 904(2):114.

Montes, M., Trujillo, I., Infante-Sainz, R., Monelli, M., and Borlaff, A. S. (2021). A Disk and No Signatures of Tidal Distortion in the Galaxy "Lacking" Dark Matter NGC 1052-DF2. , 919(1):56.

Neumayer, N., Seth, A., and Böker, T. (2020). Nuclear star clusters. , 28(1):4.

Prugniel, P. and Simien, F. (1997). The fundamental plane of early-type galaxies: non-homology of the spatial structure. , 321:111–122.

Read, J. I., Goerdt, T., Moore, B., Pontzen, A. P., Stadel, J., and Lake, G. (2006). Dynamical friction in constant density cores: a failure of the Chandrasekhar formula. , 373(4):1451–1460.

Saifollahi, T., Zaritsky, D., Trujillo, I., Peletier, R. F., Knapen, J. H., Amorisco, N., Beasley, M. A., and Donnerstein, R. (2022). Implications for galaxy formation models from observations of globular clusters around ultra-diffuse galaxies. , 511(3):4633–4659.

Secker, J. and Harris, W. E. (1993). A Maximum-Likelihood Analysis of Globular Cluster Luminosity Distributions in the Virgo Ellipticals. , 105:1358.

Shen, Z., van Dokkum, P., and Danieli, S. (2021). A Complex Luminosity Function for the Anomalous Globular Clusters in NGC 1052-DF2 and NGC 1052-DF4. , 909(2):179.

Shen, Z., van Dokkum, P., and Danieli, S. (2023). Confirmation of an Anomalously Low Dark Matter Content for the Galaxy NGC 1052-DF4 from Deep, High-resolution Continuum Spectroscopy. , 957(1):6.

Terzić, B. and Graham, A. W. (2005). Density-potential pairs for spherical stellar systems with Sérsic light profiles and (optional) power-law cores. , 362(1):197–212.

Tremaine, S. D., Ostriker, J. P., and Spitzer, L., J. (1975). The formation of the nuclei of galaxies. I. M31. , 196:407–411.

Trujillo, I., Beasley, M. A., Borlaff, A., Carrasco, E. R., Di Cintio, A., Filho, M., Monelli, M., Montes, M., Román, J., Ruiz-Lara, T., Sánchez Almeida, J., Valls-Gabaud, D., and Vazdekis, A. (2019). A distance of 13 Mpc resolves the claimed anomalies of the galaxy lacking dark matter. , 486(1):1192–1219.

Trujillo, I., Roman, J., Filho, M., and Sánchez Almeida, J. (2017). The Nearest Ultra Diffuse Galaxy: UGC 2162. , 836(2):191.

van der Burg, R. F. J., Hoekstra, H., Muzzin, A., Sifón, C., Viola, M., Bremer, M. N., Brough, S., Driver, S. P., Erben, T., Heymans, C., Hildebrandt, H., Holwerda, B. W., Klaes, D., Kuijken, K., McGee, S., Nakajima, R., Napolitano, N., Norberg, P., Taylor, E. N., and Valentijn, E. (2017). The abundance of ultra-diffuse galaxies from groups to clusters. UDGs are relatively more common in more massive haloes. , 607:A79.

van Dokkum, P., Abraham, R., Brodie, J., Conroy, C., Danieli, S., Merritt, A., Mowla, L., Romanowsky, A., and Zhang, J. (2016). A High Stellar Velocity Dispersion and ∼100 Globular Clusters for the Ultra-diffuse Galaxy Dragonfly 44. , 828(1):L6.

van Dokkum, P., Danieli, S., Abraham, R., Conroy, C., and Romanowsky, A. J. (2019). A Second Galaxy Missing Dark Matter in the NGC 1052 Group. , 874(1):L5.

van Dokkum, P., Danieli, S., Abraham, R., Conroy, C., and Romanowsky, A. J. (2019). A second galaxy missing dark matter in the ngc 1052 group. *The Astrophysical Journal Letters*, 874(1):L5.

van Dokkum, P., Danieli, S., Cohen, Y., Merritt, A., Romanowsky, A. J., Abraham, R., Brodie, J., Conroy, C., Lokhorst, D., Mowla, L., O'Sullivan, E., and Zhang, J. (2018a). A galaxy lacking dark matter. , 555(7698):629–632.

van Dokkum, P., Danieli, S., Cohen, Y., Merritt, A., Romanowsky, A. J., Abraham, R., Brodie, J., Conroy, C., Lokhorst, D., Mowla, L., O'Sullivan, E., and Zhang, J. (2018b). A galaxy lacking dark matter. , 555(7698):629–632.

van Dokkum, P. G., Abraham, R., Merritt, A., Zhang, J., Geha, M., and Conroy, C. (2015a). Forty-seven Milky Way-sized, Extremely Diffuse Galaxies in the Coma Cluster. , 798(2):L45.

van Dokkum, P. G., Romanowsky, A. J., Abraham, R., Brodie, J. P., Conroy, C., Geha, M., Merritt, A., Villaume, A., and Zhang, J. (2015b). Spectroscopic Confirmation of the Existence of Large, Diffuse Galaxies in the Coma Cluster. , 804(1):L26.

Villegas, D., Jordán, A., Peng, E. W., Blakeslee, J. P., Côté, P., Ferrarese, L., Kissler-Patig, M., Mei, S., Infante, L., Tonry, J. L., and West, M. J. (2010). The acs fornax cluster survey. viii. the luminosity function of globular clusters in virgo and fornax early-type galaxies and its use as a distance indicator*. , 717(2):603.

Virtanen, P., Gommers, R., Oliphant, T. E., Haberland, M., Reddy, T., Cournapeau, D., Burovski, E., Peterson, P., Weckesser, W., Bright, J., van der Walt, S. J., Brett, M., Wilson, J., Millman, K. J., Mayorov, N., Nelson, A. R. J., Jones, E., Kern, R., Larson, E., Carey, C. J., Polat, İ., Feng, Y., Moore, E. W., VanderPlas, J., Laxalde, D., Perktold, J., Cimrman, R., Henriksen, I., Quintero, E. A., Harris, C. R., Archibald, A. M., Ribeiro, A. H., Pedregosa, F., van Mulbregt, P., and SciPy 1.0 Contributors (2020). SciPy 1.0: Fundamental Algorithms for Scientific Computing in Python. *Nature Methods*, 17:261–272.

Yagi, M., Koda, J., Komiyama, Y., and Yamanoi, H. (2016). Catalog of Ultra-diffuse Galaxies in the Coma Clusters from Subaru Imaging Data. , 225(1):11.

Zaritsky, D. and Behroozi, P. (2022). Photometric mass estimation and the stellar mass–halo mass relation for low mass galaxies. , 519(1):871–883.